

Spectrophotometric follow-up of GU Mus, the (X-ray) Nova Muscae 1991^{*}

M. Della Valle, N. Masetti, and A. Bianchini

Dipartimento di Astronomia, Università di Padova, Vicolo dell'Osservatorio 5, I-35122 Padua, Italy

Received 25 February 1997 / Accepted 14 August 1997

Abstract. The spectrophotometric follow-up of the X-ray nova GU Mus (=GS 1124-68) is presented. We have analysed 128 *B*, *V* and *R* frames and 19 optical spectra, collected at ESO-La Silla, from the epoch of the discovery to January 1992. The optical lightcurve appears to be typical for a X-ray nova and exhibits secondary maxima in coincidence with the X-ray ones. The spectra show that Balmer and He II $\lambda 4686$ emission lines and the N III $\lambda 4640$ emission blend widen during the decline. A possible explanation of this behaviour is proposed and applied to the spectral evolution of other X-ray novae.

Key words: accretion disks – stars: individual (GU Mus, GS 1124-68) – X-rays: stars

1. Introduction

Soft X-ray Transients (or SXTs) form a small subclass of Low Mass X-ray Binaries (LMXBs) and are composed of a late type low-mass star (usually a dwarf or a subgiant) which loses matter via Roche-lobe overflow onto a massive collapsed primary. The importance of these systems lies in the fact that about 80% of them are suspected to harbor a black hole. This has been demonstrated in 6 cases: V616 Mon (McClintock & Remillard 1986), GU Mus (Remillard et al. 1992), GRO J1655-40 (Bailyn et al. 1995b), V2107 Oph (Remillard et al. 1996), QZ Vul (Casares et al. 1995) and V404 Cyg (Casares et al. 1992), whose mass functions exceed $3 M_{\odot}$.

GS 1124-68 (=X-Ray Nova Muscae 1991) was discovered as a bright transient X-ray source on January 8, 1991 by the Ginga (Makino 1991) and the GRANAT (Lund & Brandt 1991) satellites. The analysis of the two-component X-ray spectrum during the outburst (Kitamoto et al. 1992, Grebenev et al. 1992, Ebisawa et al. 1994) allowed the classification of this object as SXT.

Its optical counterpart, GU Mus, was discovered by Della Valle et al. (1991) one week later, on January 15, 1991. GU

Mus increased its luminosity from $V \sim 20.5$ to $V \sim 13.5$, a brightening of ~ 7 mag which is typical of X-ray novae (van Paradijs & McClintock 1995). The optical spectrum at maximum (Della Valle et al. 1991) showed Balmer, He I, He II, N II and N III emission features superimposed on a blue optical continuum, thus resembling those of outbursting Dwarf Novae (DNe). From these observations a color excess of 0.30 mag was derived, confirmed later on by the analysis of UV spectra (Cheng et al. 1992). In addition, Ball et al. (1995) detected a transient radio emission during maximum, which is another typical feature of outbursting SXTs.

X-ray and optical observations during the decay showed two important behaviours: the presence of an electron-positron annihilation line at 0.511 MeV (Sunyaev et al. 1992, Goldwurm et al. 1992), which is considered a clue for the presence of a black hole (see the review by Tanaka & Lewin 1995), and the appearance of superhumps (Bailyn 1992). The latter phenomenon, first seen in SU UMa-type DNe, takes place only if the mass ratio $q = M_2/M_1$ is less than 0.25-0.33 (Whitehurst & King 1991). Since the mass of the secondary in SXTs is $\gtrsim 0.5 M_{\odot}$ (van Paradijs & McClintock 1995, Tanaka & Lewin 1995), the accretor should be a highly-collapsed object. Actually, superhumps in SXTs have been observed in outbursting QZ Vul (Charles et al. 1991), V518 Per (Kato et al. 1995), V2293 Oph (Masetti et al. 1996) and MM Vel (Masetti et al. 1997; Della Valle et al. 1997).

The X-ray lightcurve also showed two secondary maxima at ~ 70 (Kitamoto et al. 1992) and ~ 200 days (Ebisawa et al. 1994) after the main X-ray peak. On the contrary, until now there is no indication of optical secondary maxima or minioutbursts.

GU Mus reverted to quiescence about one year after the outburst (Della Valle 1992). In April 1992, when the star was already at minimum, Remillard et al. (1992), found that the mass function of the primary is $\sim 3 M_{\odot}$, which is already beyond the maximum allowed mass for a neutron star (Rhodes & Ruffini 1974). This value placed GU Mus amongst the galactic black-hole candidates.

In this paper we present the spectrophotometric follow-up of GU Mus, from the discovery to the late decline. Sect. 2 illustrates the observations and the reduction of images and spectra. Sect.

Send offprint requests to: Nicola Masetti (masetti@astrpd.pd.astro.it)

^{*} Based on observations obtained at the European Southern Observatory, La Silla, Chile.

Table 1. The journal of the observations. The upper part of the Table lists the photometric data, while the spectroscopic observations are reported in the lower part

Date	Telescope	Filter or passband	Number of frames	Exp. times (minutes)
Imaging				
Jan. 15, 1991	2.2m,NTT	<i>B, V, R</i>	2,2,3	0.083,0.16,0.25,0.5
Jan. 16, 1991	2.2m	<i>B, V, R</i>	1,1,2	0.16,0.33
Jan. 17, 1991	2.2m	<i>B, V, R</i>	1,1,1	0.16,0.5
Jan. 18, 1991	2.2m	<i>B, V, R</i>	1,1,1	0.25,0.5
Jan. 19, 1991	2.2m	<i>B, V, R</i>	1,1,1	0.42,0.66
Jan. 20, 1991	2.2m	<i>B, V, R</i>	1,1,1	0.42,0.66
Jan. 21, 1991	2.2m	<i>B, V, R</i>	1,1,1	0.42,0.66
Jan. 22, 1991	2.2m	<i>B, V, R</i>	1,1,1	0.42,0.66
Jan. 23, 1991	NTT	<i>V, R</i>	1,1	0.16,0.33
Jan. 24, 1991	NTT	<i>V, R</i>	1,2	0.2,0.42
Jan. 29, 1991	2.2m	<i>B, V, R</i>	15,1,1	0.5,1
Feb. 11, 1991	NTT	<i>R</i>	2	0.083,0.5
Feb. 17, 1991	2.2m	<i>B, V, R</i>	1,1,3	0.16,0.33
Feb. 18, 1991	2.2m	<i>B, V, R</i>	2,2,3	0.16,0.33
Feb. 19, 1991	2.2m	<i>B, V, R</i>	1,1,1	0.25,0.5
Feb. 21, 1991	3.6m	<i>B, V, R</i>	1,1,1	0.13,0.25
Feb. 24, 1991	Danish	<i>B, V, R</i>	3,1,2	0.25,0.33,0.5,5,10
Feb. 28, 1991	NTT	<i>B, V, R</i>	2,1,1	0.1,0.15,0.33
Mar. 1, 1991	NTT	<i>B, V, R</i>	1,1,1	0.1,0.33
Mar. 2, 1991	NTT	<i>B, V, R</i>	1,1,1	0.1,0.33
Mar. 6, 1991	NTT	<i>B, V, R</i>	1,1,1	0.1,0.25
Mar. 12, 1991	Danish	<i>B, V</i>	3,3	0.66,1.33
Mar. 13, 1991	Danish	<i>B, V</i>	2,2	0.66,1.33
Mar. 14, 1991	Danish	<i>B, V</i>	3,3	0.66,1.33
Mar. 16, 1991	Danish	<i>B, V</i>	1,4	0.66,1.33
Mar. 17, 1991	Danish	<i>B, V</i>	2,2	0.66,1.33
Mar. 18, 1991	Danish	<i>B, V</i>	2,2	0.66,1.33
Mar. 25, 1991	NTT	<i>B, V, R</i>	1,1,1	0.16,0.5
May 19, 1991	3.6m	<i>B, V, R</i>	1,1,1	0.5,1.5
Jan. 1, 1992	NTT	<i>B, V, R</i>	1,1,1	1,2,3
Spectra				
Jan. 15, 1991	NTT	#3	2	3
Jan. 18, 1991	1.5m	<i>Gr15,Gr17</i>	1,1	15,18.3
Jan. 19, 1991	1.5m	<i>Gr15,Gr17</i>	1,1	25,40
Jan. 20, 1991	1.5m	<i>Gr17</i>	1	50
Jan. 23, 1991	NTT	#5	1	10
Feb. 15, 1991	1.5m	3750-7500 Å	1	20
Feb. 21, 1991	1.5m	3500-10100 Å	1	15
Mar. 6, 1991	NTT	#2, <i>Gr5</i>	1,1	10,30
Mar. 21, 1991	2.2m	#7	1	30
Mar. 25, 1991	NTT	#5,#6	2,1	10,20
May 5, 1991	1.5m	<i>Gr21</i>	1	20
May 19, 1991	3.6m	<i>B300,R300</i>	1,1	10,15

3 shows the analysis of the data, and Sect. 4 discusses the results and draws the conclusions.

2. Observations and data reduction

All the images and the spectra were taken at La Silla with different ESO telescopes. Table 1 gives the complete journal of observations. The upper part of Table 1 lists the images, while the lower part reports the spectroscopic observations.

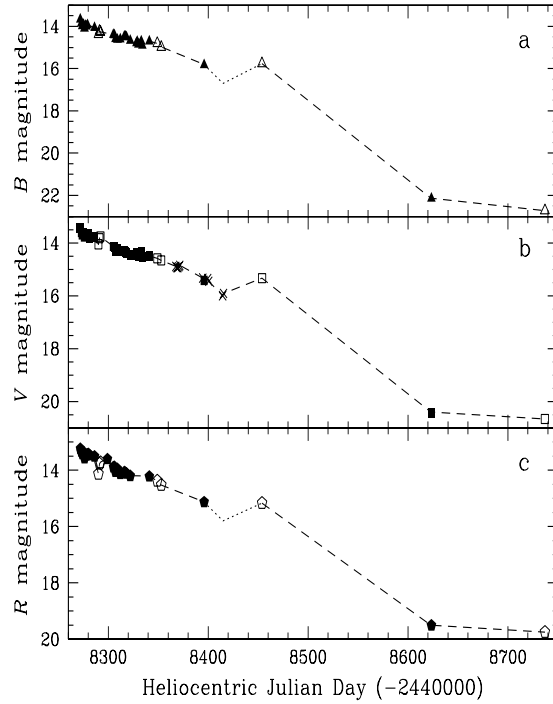


Fig. 1. **a** *B*, **b** *V* and **c** *R* lightcurves of the outburst of GU Mus. We indicate, with a different hyphenation, the possible presence in the *B* and *R* bands of the secondary maximum seen in the *V* lightcurve ~ 200 days after the X-ray peak. Open symbols indicate the magnitude determinations made by King et al. (1996), while crosses correspond to the nightly means of the observations made by Bailyn (1992)

We have globally obtained 128 images (53 in the *B*, 41 in the *V* and 34 in the *R* Johnson bands) and 19 spectra (with slit widths varying from 1'' to 2''), giving a resolution between 2.0 and 9.6 Å/pixel) over a period of nearly one year (from January 15, 1991 to January 1, 1992). However most observations are concentrated within the first three months after the outburst. Standard bias and flat field corrections were performed on each frame.

Images were reduced with DAOPHOT II (Stetson 1987) and ALLSTAR inside MIDAS. The nova has been calibrated in *B* and *V* magnitudes by using the field stars 1, 2 and 3 (Bailyn 1992). We have measured the *R* magnitudes of these three stars through Mark A and T Phe Landolt fields (Landolt 1992), and obtained $R = 13.20 \pm 0.02$, $R = 14.49 \pm 0.02$ and $R = 14.54 \pm 0.02$, respectively. Table 2 reports the *B*, *V* and *R* magnitudes of the object, together with the $(B - V)$ and $(V - R)$ color indexes. The typical photometric error for each measurement is of the order of ± 0.05 mag in the *B* band and ± 0.03 mag in both *V* and *R*.

The reduction of the spectroscopic material was carried out with IRAF. He-Ar lamps were used for the wavelength calibration, and the standards Feige 56, EG 76, L970-30, LTT 3218, Hiltner 600, CD-32, Wolf 485A and EG 274 for the flux calibration. We corrected the spectra for interstellar reddening with the prescription of Cardelli et al. (1989), and using $E(B - V) = 0.30$ as derived by Della Valle et al. (1991).

Table 2. B , V and R magnitudes, along with the $(B - V)$ and $(V - R)$ colors, of GU Mus. The typical error is ± 0.05 mag for the B values and ± 0.03 mag for V and R . When more than one measurement in the same band was available during the same night, the mean value has been reported. The magnitudes are referred to the mean Heliocentric Julian Day (HJD) of the observations

HJD	B	V	R	$(B - V)$	$(V - R)$
2448271.73	13.66	13.43	13.24	0.23	0.19
2448272.72	13.84	13.60	13.33	0.24	0.27
2448273.68	13.97	13.68	13.42	0.29	0.26
2448274.84	13.91	13.62	13.36	0.29	0.26
2448275.86	14.07	13.77	13.57	0.30	0.20
2448276.86	13.94	13.67	13.41	0.27	0.26
2448277.87	13.97	13.71	13.46	0.28	0.25
2448278.85	13.92	13.63	13.43	0.29	0.20
2448279.80	–	13.64	13.41	–	0.23
2448280.75	–	13.80	13.46	–	0.24
2448285.83	14.05	13.75	13.51	0.30	0.24
2448298.87	–	–	13.60	–	–
2448304.78	14.38	14.13	13.88	0.25	0.25
2448305.77	14.39	14.12	13.87	0.27	0.25
2448306.90	14.57	14.29	14.04	0.28	0.25
2448308.85	14.60	14.23	13.95	0.37	0.28
2448311.77	14.60	14.30	14.12	0.30	0.18
2448315.75	14.46	14.30	14.06	0.16	0.24
2448316.78	14.45	14.31	14.08	0.14	0.23
2448317.80	14.49	14.37	14.10	0.12	0.27
2448321.63	14.66	14.46	14.20	0.20	0.26
2448327.74	14.78	14.45	–	0.33	–
2448328.73	14.71	14.36	–	0.35	–
2448329.74	14.83	14.47	–	0.36	–
2448331.75	14.80	14.45	–	0.35	–
2448332.70	14.69	14.34	–	0.35	–
2448333.71	14.88	14.53	–	0.35	–
2448340.73	14.69	14.48	14.21	0.21	0.27
2448395.51	15.81	15.40	15.12	0.41	0.28
2448622.85	22.1 ± 0.3	20.5 ± 0.1	19.5 ± 0.1	1.6 ± 0.3	1.0 ± 0.15

Finally, the observation times have been corrected to heliocentric times of mid-exposure.

3. Data analysis

3.1. Photometry

The lightcurves in B , V and R bands are shown in Fig. 1a,b,c. Light fluctuations are seen in each lightcurve, with amplitudes up to 0.2 mag. These light variations are erratic in the early decline, and later they appear as small light oscillations with typical timescales of about 10 days (see also Fig. 5a).

Fig. 2 reports the X-ray and the B lightcurves in a common flux scale. The comparison between the X-ray peak flux (Kitamoto et al. 1992) and the optical flux computed from the spectra at maximum light (see Fig. 3) leads to a ratio of $\sim 10^3$, which is typical for LMXBs and outbursting SXTs (Tanaka & Lewin 1995).

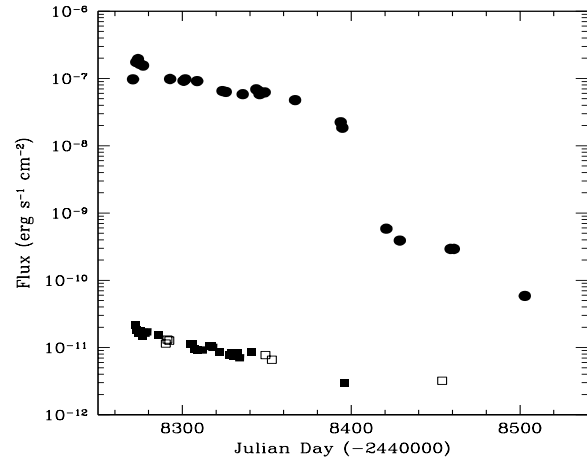


Fig. 2. X-ray (circles) and B (squares) lightcurves of the outburst of GU Mus. X-ray data are extracted from Table 2 of Ebisawa et al. (1994). Open squares indicate the B magnitude determinations made by King et al. (1996). Note their similar trends and the coincidence of their secondary maxima

Table 3. Decay rates (in mag d^{-1}) of the B , V and R outburst lightcurves of GU Mus computed at different phases of the decline

Decline phase	B	V	R
January 1991	0.0199	0.0161	0.0135
Feb.-Mar. 1991	0.0109	0.0091	0.0090
Apr.-May 1991	0.0203	0.0168	0.0166
May 1991-Jan. 1992	0.0278	0.0220	0.0193
Jan. 1991-Jan. 1992	0.0241	0.0199	0.0178

A linear fit on the decay lightcurves has been performed to estimate the decline rates in the B , V and R bands. Table 3 reports the decay rates for each photometric band in different parts of the lightcurve.

Two bumps at ~ 50 and ~ 70 days after the maximum are clearly visible (see also Fig. 5a). The second bump is consistent with the secondary maximum observed in the X-ray band (see Fig. 2) and reported by Kitamoto et al. (1992), while the first one might be associated to a small feature in the X-ray lightcurve (see Fig. 1, upper panel, of Kitamoto et al. 1992; see also Fig. 4 of Greiner et al. 1994). This behaviour is typical of SXTs during the decline (Chen et al. 1993, van Paradijs & McClintock 1995).

The decay starts again in the April-May period, and strengthens in the second part of 1991. It can be also noticed from Table 3 that, after March 1991, the decay in the B is slightly faster than the ones in V and R .

However, if we integrate our photometric data with the magnitude determinations reported by King et al. (1996) and with the nightly averages of the Bailyn's (1992) observations, we notice another local maximum in the V lightcurve around Julian Day (hereafter JD) 2448460, i.e. ~ 200 days after the X-ray peak: thus, the increased luminosity can be correlated with the tertiary X-ray maximum (see Fig. 2) observed by Ebisawa et al. (1994).

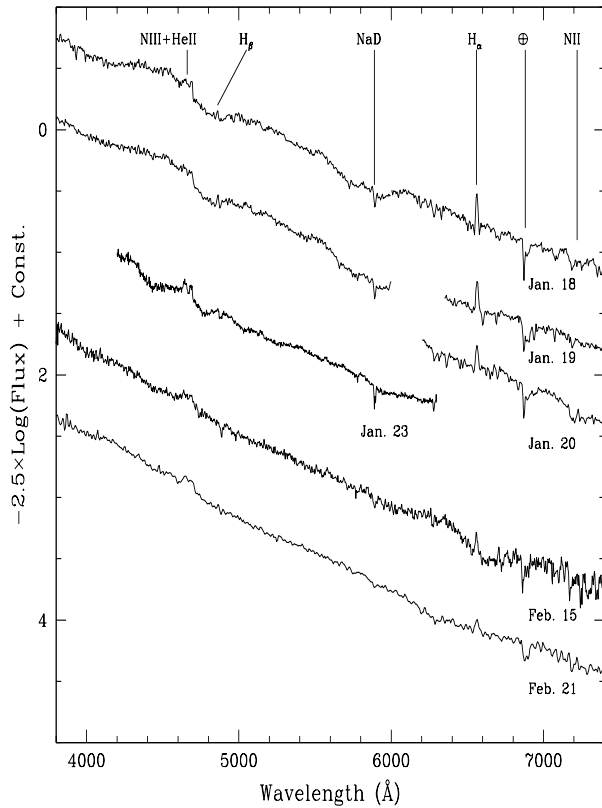


Fig. 3. Six spectra of GU Mus acquired between January and February 1991 and listed in Table 1. The main spectroscopic features are indicated. Fluxes are in units of $\text{erg s}^{-1} \text{cm}^{-2}$. For sake of clarity, the spectra have been separated by 0.5 logarithmic flux units. The additive constant for the spectrum at the top of the figure is -33.5

The presence of minioutbursts during the late decline of MM Vel (=X-Ray Nova Velorum 1993; Bailyn & Orosz 1995) and V518 Per (=GRO J0422+32; Chevalier & Ilovaisky 1995, Callanan et al. 1995), would indicate that they are a not unusual feature in these objects, though for these two systems this phenomenon has been purely optical and not associated with a restart of the X-ray activity.

The magnitudes at minimum, as measured on January 1, 1992 (see Table 2), are in agreement with the mean magnitude determinations by Remillard et al. (1992) and by King et al. (1996).

The evolution of $(B-V)$ and $(V-R)$ colors during the decay is shown in Table 2. It is noteworthy that, while the $(V-R)$ color is roughly constant around 0.25 from the beginning of the outburst until mid-May 1991, the $(B-V)$ seems to decay ($0.00118 \text{ mag d}^{-1}$) as the decline proceeds. The mean $(B-V)$ color fairly agrees with the value given by Bailyn (1992) for the month of April 1991. We also note that the object appears to become bluer around JD 2448320 and ~ 20 -25 days later, that is during the two bumps in the early B lightcurve (see Fig. 5a).

At the beginning of January 1992, the colors return to their pre-outburst values (see Della Valle et al. 1991).

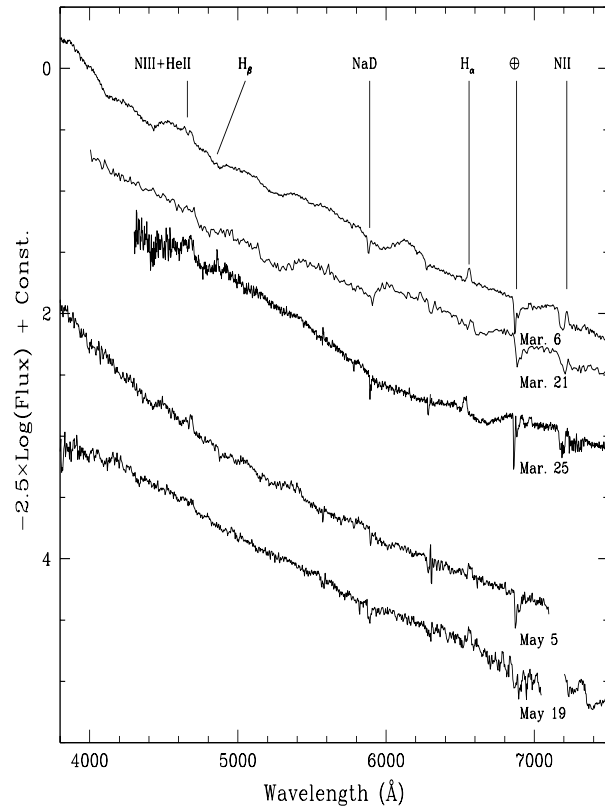


Fig. 4. Five spectra of GU Mus taken between March and May 1991 and listed in Table 1. The main spectroscopic features are indicated. Fluxes are in units of $\text{erg s}^{-1} \text{cm}^{-2}$. For sake of clarity, the spectra have been separated by 0.5 logarithmic flux units. The additive constant for the spectrum at the top of the figure is -33.5

3.2. Spectroscopy

The spectra taken during the follow-up period are listed in Table 1 and shown in Figs. 3 and 4.

The most prominent emission lines are H_{α} , H_{β} , the N III+He II blend at 4640 - 4686 \AA and, from March 1991 (Fig. 4; first spectrum from top), N II $\lambda 7217$. The fluxes of these emission lines are reported in Table 4. The only evident absorption lines are the interstellar NaD doublet at 5890 \AA and the telluric lines at 6850 \AA and 7600 \AA (the latter has not been included in the figures).

The mean value of the EW of the NaD absorption is $1.4 \pm 0.1 \text{ \AA}$, in good agreement with the estimate of Della Valle et al. (1991). According to the relation between the EW of NaD and the $(B-V)$ color excess given by Barbon et al. (1990), we find $(B-V)_0 \sim +1.3$ at quiescence, consistent with the spectral classification by Remillard et al. (1992) and by Orosz et al. (1996).

Fig. 5 shows the first part of the B lightcurve decline together with EW's and FWHM's of the main emission lines visible in the spectra of Figs. 3 and 4.

The spectral evolution of the nova during the decline is mainly characterized by the weakening and the broadening of

Table 4. Fluxes (in units of 10^{-15} erg s $^{-1}$ cm $^{-2}$) of the main emission features seen in the spectra of Figs. 3 and 4.

Decline phase	H $_{\alpha}$	H $_{\beta}$	He II	N III	N II
Jan. 18	78 \pm 8	43 \pm 4	99 \pm 9	180 \pm 20	–
Jan. 19	71 \pm 7	46 \pm 5	90 \pm 8	150 \pm 15	–
Jan. 20	55 \pm 6	(abs.)	–	–	18 \pm 2
Jan. 23	–	(abs.)	94 \pm 9	170 \pm 20	–
Feb. 15	56 \pm 6	–	74 \pm 7	120 \pm 10	–
Feb. 21	20 \pm 3	–	58 \pm 9	75 \pm 10	–
Mar. 6	18 \pm 3	9 \pm 2	37 \pm 6	48 \pm 7	16 \pm 3
Mar. 21	28 \pm 4	–	36 \pm 5	54 \pm 8	–
Mar. 25	24 \pm 4	46 \pm 7	160 \pm 30	83 \pm 10	16 \pm 3
May 5	8 \pm 2	–	27 \pm 5	13 \pm 3	–
May 19	10 \pm 2	–	16 \pm 3	12 \pm 3	–

the H $_{\alpha}$ emission, as shown in Fig. 5b,c. An increase of the FWHM's is actually observed also in the He II λ 4686 emission, while the behaviour of the λ 4640 blend is more uncertain due to the broadened profile and to the bad signal-to-noise ratio (see Fig. 5c). On February 21 and on March 21, H $_{\alpha}$ seems to be embedded inside a wide and shallow absorption. This is not unusual for SXTs (see e.g. Callanan et al. 1995, Masetti et al. 1997, Bianchini et al. 1997).

The profile of H $_{\beta}$, close to maximum light, shows a shallow absorption filled in by an emission core. During the secondary X-ray maximum (Fig. 4; third spectrum from top) only the emission component is shown.

The He II and λ 4640 blend fluxes decay monotonically with time but rise up during the X-ray ‘reflare’. At that time (see Fig. 5b,c) also the EW and FWHM of He II show a ‘jump’.

The N II is clearly present only in the March spectra (in Fig. 4), and perhaps in the spectrum of January 20 (Fig. 3; third spectrum from top), with an average EW of ~ 2 Å.

The continuum becomes less steep in the blue part as the outburst proceeds; actually, the last spectrum of the run appears flatter than the other ones. At this stage, the disk emission is still predominant, indeed we do not see any absorption feature of the secondary, since the magnitude of the system is still around $V \sim 15.5$ and the secondary is a K3-K5 dwarf (Orosz et al. 1996).

4. Discussion

4.1. The lightcurves

We have detected a bump in the B and ($B - V$) lightcurves very close to the secondary X-ray maximum (see Fig. 5a; see also Fig. 2), and a brightening in the V band (and possibly also in B and R) close to the tertiary X-ray maximum at ~ 200 days after the peak.

It is noteworthy that these minioutbursts are different from those shown by MM Vel (Bailyn & Orosz 1995) and by V518 Per (Chevalier & Ilovaisky 1995) because the latter objects show purely optical ‘reflares’ well after the end of the X-ray outburst which have no X-ray counterpart.

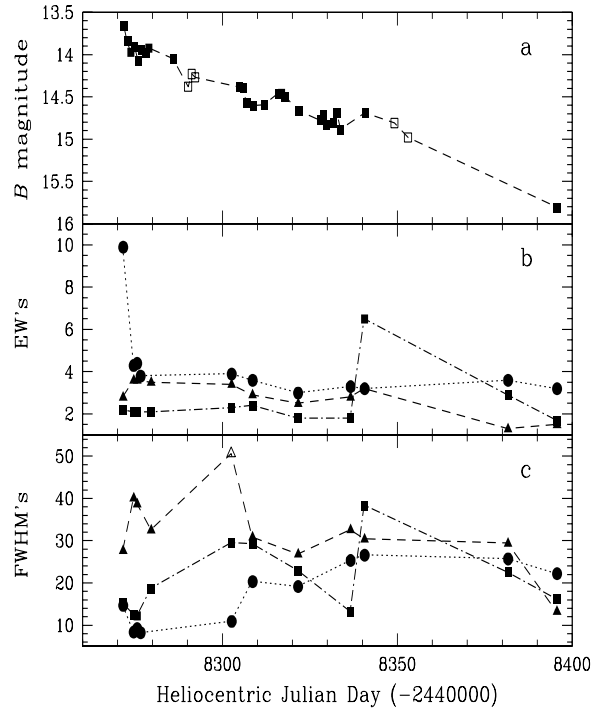


Fig. 5a–c. Evolution of the B magnitude (a), EW’s (b) and FWHM’s (c) of H $_{\alpha}$ (circles), He II λ 4686 (squares) and N III λ 4640 blend (triangles) between January and May 1991. EW’s and FWHM’s are both given in Å. The empty triangle in the lower panel corresponds to a rather uncertain measurement, while the open squares in the upper panel indicate the observations of King et al. (1996)

From Table 3 we also note that the decay is slower as we move to higher wavelengths: this may be due to the cooling of the X-ray illuminated zones of the binary system (i.e., the outer disk and the inner face of the secondary).

The light fluctuations observed during the first decline (Fig. 5a) might be due to a superhump activity which could have been present also before it was observed by Bailyn (1992).

Other longer-term light fluctuations, observed during the decline, might be real and correspond to faint secondary maxima. In particular, a sort of 10-day periodicity appears to be present during the decline in the B lightcurve (Fig. 5a). According to Warner (1995; and references therein), this behaviour is similar to that shown by some classical novae during the transition phase.

4.2. The spectra and the disk stability

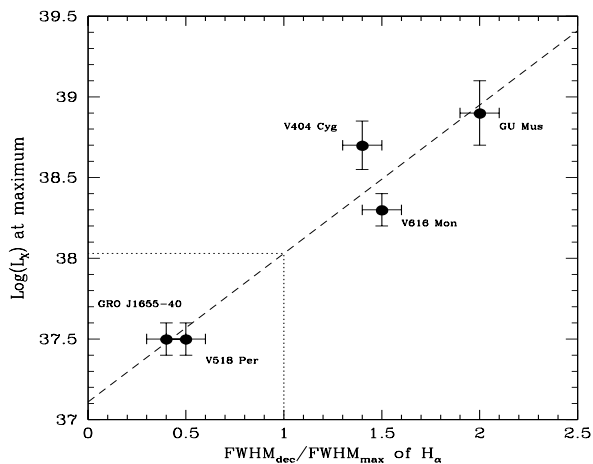
During the first five days of the decline the EW of H $_{\alpha}$ drops quite steeply by a factor 2.5, then it remains at about the same value throughout the first half of 1991.

The He II line shows a bump which approximately starts at JD 2448340, in coincidence with the secondary maximum of the X-ray (Kitamoto et al. 1992) and the B lightcurves. The increase of luminosity in the high-energy bands (UV and X-rays) should then be responsible for this bump, since the strength of this

Table 5. Optical decline rates, distances, time from the X-ray peak at which the FWHM_{dec} of $\text{H}\alpha$ was measured and corresponding magnitude drops (Δm) for the 5 SXTs quoted in Sect. 4.2

Object	Optical decline rate (mag d^{-1})	Distance (kpc)	Δt	Δm	Ref. No.
V518 Per	0.009	2	~ 200	~ 2	1,2,3
V616 Mon	0.015	1.05	~ 200	~ 3	4,5
GU Mus	0.016	5.5	~ 150	~ 2.5	6,7
GRO J1655-40	0.016	3.2	~ 200	~ 3	8,9,10,11
V404 Cyg	0.009	2.6	~ 180	~ 2	8,12

References. – 1. Castro-Tirado et al. 1993; 2. Chevalier & Ilovaisky 1995; 3. Shrader et al. 1994; 4. Whelan et al. 1977; 5. Shahbaz et al. 1994; 6. this work; 7. Orosz et al. 1996; 8. Goranskij et al. 1996; 9. Hjellming & Rupen 1995; 10. Bailyn et al. 1995a; 11. Bianchini et al. 1997; 12. Casares et al. 1993.

**Fig. 6.** Correlation between the X-ray luminosity (in erg s^{-1}) at maximum and the ratio of FWHM's of $\text{H}\alpha$ emission at mid-decline and at the beginning of the outburst for 5 SXTs. The long-dashed line represents the least-squares fit of the data points

emission line is actually correlated with the UV continuum level (Garnett et al. 1991). Later on, the He II line becomes weaker, as also shown by Cheng et al. (1992; their Fig. 3c).

The EW of the $\lambda 4640$ blend appears slightly stronger than that of He II before JD 2448340 and it seems to remain at about the same level throughout the brightening of the He II component. It shows no increase when the X-ray and the B lightcurves have a secondary maximum (see Fig. 2 and Fig. 5a,b). This behaviour could be explained by the rather broadened and undefined profile of the $\lambda 4640$ blend and/or by its lower excitation potential with respect to that of He II .

The FWHM (Fig. 5c) of $\text{H}\alpha$ and of He II tend to increase with time. The FWHM of the $\lambda 4640$ blend starts with larger values, and then it seems to decrease. The widening at JD 2448304 shown in Fig. 5c is rather uncertain due to the difficult determination of the profile. The FWHM's of He II and of the $\lambda 4640$ blend seem to decrease beginning on May 19, 1991. Anyway, the lack of spectroscopic observations after May 19, 1991 does not allow us to fully confirm this trend. This fact would indicate

that during the decline the emission region moves inward in the disk, that is, towards larger keplerian velocity radii.

However we note that X-ray novae may present opposite behaviours. Some objects, like V518 Per (Shrader et al. 1994) and GRO J1655-40 (Bianchini et al. 1997), show emission lines with decreasing widths with the time; some other ones, like GU Mus (this work), V404 Cyg (Gotthelf et al. 1992) and V616 Mon (Whelan et al. 1977) show emission lines which become larger and larger during the decline.

To investigate this point we plot in Fig. 6 the ratio $\text{FWHM}_{\text{dec}}/\text{FWHM}_{\text{max}}$ of the $\text{H}\alpha$ line, at about 150-200 days after the X-ray peak and at maximum, versus the X-ray luminosity at maximum of the 5 SXTs with available data (in Table 5), i.e. GU Mus (this work), V404 Cyg (Gotthelf et al. 1992), V616 Mon (Whelan et al. 1977), GRO J1655-40 (Bianchini et al. 1997) and V518 Per (Shrader et al. 1994). The errors on $\text{Log}(L_X)$ are mainly due to the uncertainty on the distance of the objects (see Table 5), while those affecting FWHM ratios are originated by the signal-to-noise ratio of the spectra. The long-dashed line represents the weighted least-squares fit of the data points:

$$\text{Log}(L_X) = 0.94(\pm 0.15) \frac{\text{FWHM}_{\text{dec}}}{\text{FWHM}_{\text{max}}} + 37.1(\pm 0.2). \quad (1)$$

The correlation coefficient of the data is 0.96, which indicates (admittedly on the basis of a scanty statistic), that these quantities seem to be correlated.

The regression line of Fig. 6 suggests a peak luminosity $\gtrsim 10^{38} \text{ erg s}^{-1}$ for the case $\text{FWHM}_{\text{dec}}/\text{FWHM}_{\text{max}}=1$. This value of the luminosity approximately represents the Eddington luminosity of SXTs. We note that the behaviour of the sub-Eddington objects would typically represent the one it is expected from the outburst caused by an enhancement of mass transfer from the secondary. Actually, former disk instability event has only triggered the mass transfer paroxysm. In fact, during the early outburst the disk becomes smaller because of the very large flow of low angular momentum material from the X-ray heated secondary; so we may observe larger emission lines. During the decline the disk relaxes and the emission region will expand

again towards lower keplerian velocities as it was suggested for GRO J1655-40 by Bianchini et al. (1997).

For super-Eddington objects, like GU Mus, accretion from the inner regions of the disk should be inhibited and the disk itself might be partially disrupted. More likely, we might argue that at super-Eddington accretion luminosities the disk turns its structure into a ‘geometrically thick’ one (see e.g. Frank et al. 1992), in which only the outer cooler regions can be seen at almost all inclinations. In this case, at light maximum the line emitting region is placed at quite large radii, thus producing narrower emission lines than during the decline, when a ‘standard’ disk is formed again.

Acknowledgements. We are indebted to the anonymous referee for stimulating comments. We also thank R. Canterna for his useful suggestions.

References

- Bailyn C.D., 1992, ApJ 391, 298
 Bailyn C.D., Orosz J.A., 1995, ApJ 440, L73
 Bailyn C.D., Orosz J.A., Girard T.M., 1995a, Nat 374, 701
 Bailyn C.D., Orosz J.A., McClintock J.E., Remillard R.A., 1995b, Nat 378, 157
 Ball L., Kesteven M.J., Campbell-Wilson D., Turtle A.J., Hjellming R.M., 1995, MNRAS 273, 722
 Barbon R., Benetti S., Cappellaro E., Rosino L., Turatto M., 1990, A&A 237, 79
 Bianchini A., Della Valle M., Masetti N., Margoni R., 1997, A&A 321, 477
 Callanan P.J., Garcia M.R., McClintock J.E. et al., 1995, ApJ 441, 786
 Cardelli J.A., Clayton G.C., Mathis J.S., 1989, ApJ 345, 245
 Casares J., Charles P.A., Naylor T., 1992, Nat 355, 614
 Casares J., Charles P.A., Naylor T., Pavlenko E.P., 1993, MNRAS 265, 834
 Casares J., Charles P.A., Marsh T.R., 1995, MNRAS 277, L45
 Castro-Tirado A.J., Pavlenko E.P., Shlyapnikov A.A. et al., 1993, A&A 276, L37
 Charles P.A., Kidger M.R., Pavlenko E.P., Prokofieva V.V., Callanan P.J., 1991, MNRAS 249, 567
 Chen W., Livio M., Gehrels N., 1993, ApJ 408, L5
 Cheng F.H., Horne K., Panagia N. et al., 1992, ApJ 397, 644
 Chevalier C., Ilovaisky S.A., 1995, A&A 297, 103
 Della Valle M., 1992, ESO Messenger 67, 35
 Della Valle M., Jarvis B.J., West R.M., 1991, Nat 353, 50
 Della Valle M., Benetti S., Cappellaro E., Wheeler J.C., 1997, A&A 318, 179
 Ebisawa K., Ogawa M., Aoki T. et al., 1994, PASJ 46, 375
 Frank J., King A.R., Raine D.J., 1992, *Accretion Power in Astrophysics*. Cambridge Univ. Press, Cambridge
 Garnett D.R., Kennicutt R.C., Chu Y.-H., Skillman E.D., 1991, ApJ 373, 458
 Goldwurm A., Ballet J., Cordier B. et al., 1992, ApJ 389, L79
 Goranskij V.P., Karitskaya E.A., Kurochkin N.E., Trunkovskij E.M., 1996, Astron. Lett. 22, 371
 Gotthelf E., Halpern J.P., Patterson J., Rich R.M., 1992, AJ 103, 219
 Grebenev S.A., Sunyaev R.A., Pavlinskij M.N., 1992, SvA Lett. 18, 5
 Greiner J., Hasinger G., Molendi S., Ebisawa K., 1994, A&A 285, 509
 Hjellming R.M., Rupen M.P., 1995, Nat 375, 464
 Kato T., Mineshige S., Hirata R., 1995, PASJ 47, 31
 King N.L., Harrison T.E., McNamara B.J., 1996, AJ 111, 1675
 Kitamoto S., Tsunemi H., Miyamoto S., Hayashida K., 1992, ApJ 394, 609
 Landolt A.U., 1992, AJ 104, 340
 Lund N., Brandt S., 1991, IAU Circ. 5161
 Makino F., 1991, IAU Circ. 5161
 Masetti N., Bianchini A., Bonibaker J., Della Valle M., Vio R., 1996, A&A 314, 123
 Masetti N., Bianchini A., Della Valle M., 1997, A&A 317, 769
 McClintock J.E., Remillard R.A., 1986, ApJ 308, 110
 Orosz J.A., Bailyn C.D., McClintock J.E., Remillard R.A., 1996, ApJ 468, 380
 Remillard R.A., McClintock J.E., Bailyn C.D., 1992, ApJ 399, L145
 Remillard R.A., Orosz J.A., McClintock J.E., Bailyn C.D., 1996, ApJ 459, 226
 Rhodes C.E., Ruffini R., 1974, Phys. Rev. Lett. 32, 324
 Shahbaz T., Naylor T., Charles P.A., 1994, MNRAS 268, 756
 Shrader C.R., Wagner R.M., Hjellming R.M., Han H.X., Starrfield S.G., 1994, ApJ 434, 698
 Stetson P.B., 1987, PASP 99, 191
 Sunyaev R.A., Churazov E., Gilfanov M. et al., 1992, ApJ 389, L75
 Tanaka Y., Lewin W.H.G., 1995, *Black-hole binaries*. In: X-ray Binaries, Lewin W.H.G., van Paradijs J., van den Heuvel E.P.J. (eds.), Cambridge Univ. Press, p. 126
 van Paradijs J., McClintock J.E., 1995, *Optical and ultraviolet observations of X-ray binaries*. In: X-ray Binaries, Lewin W.H.G., van Paradijs J., van den Heuvel E.P.J. (eds.), Cambridge Univ. Press, p. 58
 Warner B., 1995, *Cataclysmic Variable Stars*. Cambridge Univ. Press, Cambridge
 Whelan J.A.J., Ward M.J., Allen D.A., 1977, MNRAS 180, 657
 Whitehurst R., King A.J., 1991, MNRAS 249, 25